2.4 GaAs Heterostructures and 2D electron gas

- To determine the band structure of the heterostructure, a self consistent solution of Poisson and Schrödinger equation has to be found, usually numerically and iteratively

- A triangular quantum well forms at the $AlGaAs/GaAs$ interface, referred to as the *heterointerface*. Often, only the quantum mechanical ground state in the triangular well is populated (at low temperatures, $T \lesssim 100K$), making this one of the best experimental realizations of a 2D system in nature that we know. This 2D electron gas s often abbreviated 2DEG. Typical widths of the wave function are about 10 nm, which means there are still some observable finite size effects, particularly in large magnetic fields. It is also possible to grow another $AlGaAs$ layer below the heterointerface shown here, resulting in a square well.

- Two structures can be distinguished: one where doping over an extended z region is used, see Figure 2.8, left. The other where the doping is localized in just a few atomic layers, called δ-*doping*, see Figure 2.8, right.

- As long as the dopants are removed from the lower $GaAs/AlGaAs$ interface, it is referred to as *modulation doping*, a technique first demonstrated by Dingle in 1978.

- Choosing the right Si-doping density is an issue of fine-tuning and very sensitive. Possible problems: parallel conduction (in the dopant layer), second subband population, no electrons in well, too high or too low carrier density in well.

- Typical Al concentration is $x \sim 0.3$, putting the conduction band of $Al_{0.3}Ga_{0.7}As$ about 300 meV above the conduction band of $GaAs$ and the top of the $Al_{0.3}Ga_{0.7}As$ valence band 160 meV below the $GaAs$ valence band.

- Usually, Si is used as the dopant. It only goes into the doping region (either into the δ layer or into a larger width band within the $AlGaAs$), all the other regions are intrinsic semiconductors

- Only a fraction of the donor atoms are ionized. Part of that fraction goes into surface states, and part into the quantum/triangular well

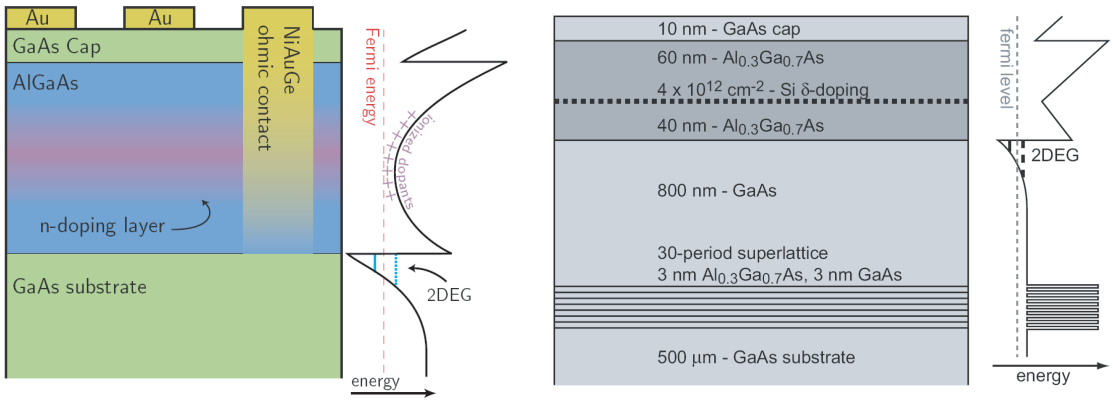

Figure 2.7: Growth profile and bandstructure of typical GaAs heterostructures.

- Two charge dipoles build up: one between surface and doping layers, and one between heterointerface and dopant layer, both resulting in electric fields between the respective layers, giving a finite but constant slope to the bands between dipoles in regions without extra charge.

- The last $GaAs$ layer making interface with vacuum is called *cap layer* and prevents oxidation that would occur was the $AlGaAs$ layer exposed to air/oxygen.

- Very large mobilities reaching $\sim 33 \times 10^6 cm^2/(Vs)$ corresponding to a mean free backscattering path of about $\sim 300\,\mu$m have been achieved.

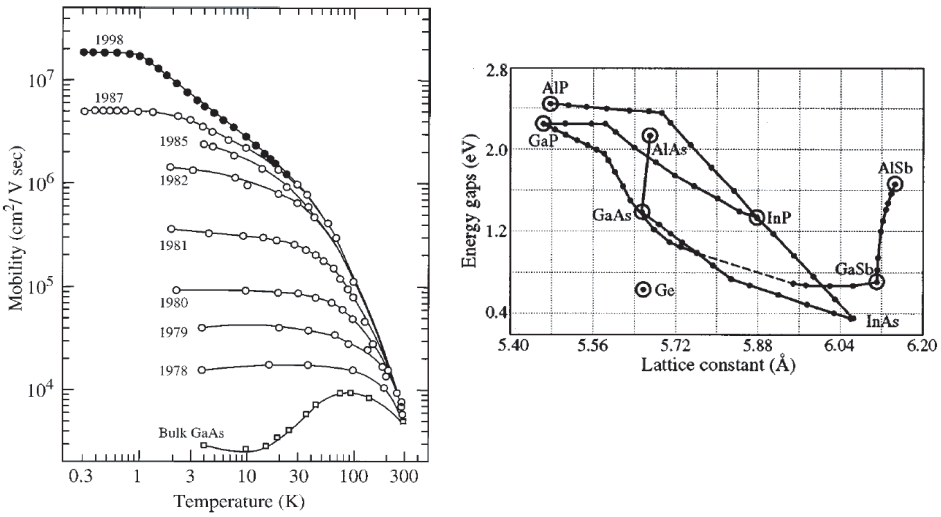

Figure 2.8: left: progress made over the years in mobility μ of electrons in a 2DEG in modulation doped GaAs/AlGaAs as a function of temperature. At high temperatures, μ is limited by scattering with phonons of the bulk. At the lowest temperatures, μ is limited by impurities and defects. [Stormer 1989] right: energy gaps as a function of the lattice constant for III-V semiconductors. [Alferov 2001]

- These very large mobilities/clean samples/long mean free paths are possible because:

  1. the heterointerface quality is excellent, not disrupting the crystal periodicity across the interface, with lattice constants of $AlGaAs$ and $GaAs$ matched within 0.5% ($AlGaAs$ condenses also into a Zinc-blende crystal). This is in stark contrast to the Si/SiO_2 interface, where the SiO_2 condenses into a highly disordered, glassy phase that is not at all matching the Si crystal, which results in severe interface scattering, reducing mobility of electrons.
  2. the ionized donors—a significant source of scattering—are spatially well separated from the 2DEG, usually between $20\,\text{nm} - 120\,\text{nm}$. Consequently, the screened Coulomb potentials the electrons see are much weaker and create predominantly small angle scattering, not very efficient at backscattering (full 180° scattering).

- By controlling the Al content the z-dependence of the band gap/band structure can be custom engineered, if desired. For example, quantum wells can be grown with a Al content quadratic in z, going from, say, 30% Al content to zero back to 30%, a so called *parabolic* well, resulting in a harmonic oscillator in the z-direction. By

top and bottom gating, the center of mass/maximum of the wave function can be shifted in the z-direction, changing the average *Al* content the electrons feel. Because the Lande g-factor depends on the *Al* concentration (it can even change sign), the g-factor can be controlled with a gate. Basically any desired potential can be grown in this way.

- By shining light on the waver, additional donors can be ionized, giving an increased density and also increased mobility, which persists over long periods of time while the sample is kept cold ($\lesssim 50\,\mathrm{K}$), often referred to as *persistent photoconductivity*.

2.5 Screening

Conduction electrons populate all states up to the Fermi energy, but the bottom of the potential is varying in a disordered manner, due to the Coulomb potentials of the ionized donor atoms and other defects and impurities. These potentials create a complicated potential mountain-valley landscape. In high mobility samples, most maxima lie below the Fermi energy, screening is efficient, and only a sparse few peaks reaching above E_F. If the density in the 2DEG is lowered, say with a top gate, then the Fermi energy correspondingly is reduced, and more peaks may appear piercing the Fermi level, giving more backscattering and a reduction in mobility. (Sometimes the analogy to the "Bath-tub potential" is made, where the water represents the electrons.)

A detailed theory of screening is left to the proper condensed matter theory lecture. Here, it be mentioned that screening can be expressed by a dielectric function $\epsilon(\omega, \vec{q})$. In Thomas-Fermi approximation, a screening length scale appears, the *Thomas-Fermi screening length*, which is usually of the order of the Fermi-wavelength. An external potential (here a Coulomb scatterer) in 3D

$$V_{ext}(r) = \frac{-Ze}{r} = \frac{-Ze^2}{(2\pi)^3} \int \frac{4\pi}{q^2} e^{\imath\vec{q}\vec{r}} d\vec{q} \tag{2.3}$$

will be screened to an effective potential electrons in the semiconductor will see:

$$V_{eff}(\vec{q}) = \frac{V_{ext}(\vec{q})}{\epsilon(\vec{q})}, \quad V_{eff}(r) = \frac{-Ze^2}{(2\pi)^3} \int \frac{1}{\epsilon(\vec{q})} \frac{4\pi}{q^2} e^{\imath\vec{q}\vec{r}} d\vec{q} \tag{2.4}$$

via a induced charge density variation that can be calculated to be:

$$\rho_{ind}(\vec{r}) = \frac{Ze}{\pi} \frac{k_{TF}^2}{k_F^2(4 + k_{TF}^2/2k_F^2)} \frac{\cos(2k_F r)}{r^3} \tag{2.5}$$

This charge density is periodically modulated with a period of half the fermi wavelength (known as *Friedel oscillations*) and decays as r^{-3} in distance (in 3D) from the scatterer. This can be understood in terms of a standing wave due to a superposition of the incoming and from the scatterer reflected waves. This is a result that depends on the dimensionality considered, indeed in 2D, as applicable for a 2DEG, one obtains:

$$V_{eff}(\vec{r}) = \frac{Ze}{\epsilon\epsilon_0} \frac{4k_T F k_F^2}{(2k_F + k_{TF})^2} \frac{\sin(2k_F r)}{2k_F r^2} \tag{2.6}$$

where the oscillations now have a longer range, decaying only as r^{-2}.

2.6 Scattering GaAs

2.6.1 Bulk GaAs scattering

Various scattering mechanisms contribute, which according to the Mathiesen rule can be added up as scattering rates to give the total scattering rate: $1/\mu = \sum_i 1/\mu_i$. Here, some scattering types are listed, first discussed for the bulk 3D GaAs case:

- impurity scattering: *neutral impurities* usually give very small scattering cross sections. Charged or *ionized impurities* represent (screened) Coulomb scatterers with peak potentials that can be comparable to the Fermi energy. At higher temperatures, electrons have larger kinetic energy and will be deflected by a smaller angle, giving larger mobility at higher temperatures. Calculations give a temperature dependence of the mobility $\propto T^{3/2}\log(T)$ in 3D.

- electron-phonon (lattice vibrations) scattering: the only scattering mechanism in perfect, pure crystals.

- electron-phonon scattering, *deformation potential*: scattering at the lattice deformation caused by phonons. Acoustic phonons are usually most relevant, which can be treated as quasi-elastic since the energy transfers are small. The temperature dependence of the corresponding mobility (scattering rate) is given by $n_{ac}/\overline{v}$, where n_{ac} is the density of acoustic phonons and $\overline{v}$ is the average electron velocity. n_{ac} is proportional to the Bose-Einstein distribution, scaling as $1/T$ at for temperatures large compared to the phonon energy and $\overline{v} \propto \sqrt{T}$, giving a mobility contribution $\propto T^{-3/2}$.

- electron-phonon scattering, *polar scattering*: *GaAs* is a polar crystal, lattice vibrations are accompanied by oscillating electric fields, particularly strong for optical phonons. For $kT \gg \hbar\omega_{op}$ where $\omega_{op} \sim 5\,\mathrm{meV}$ denotes the optical phonon energy, the resulting mobility varies as $T^{-1/2}$

- electron-phonon scattering, *piezo-electric scattering*: *GaAs* is also piezoelectric, meaning that a polarization field develops in response to a crystal deformation, also with a $T^{-1/2}$ contribution.

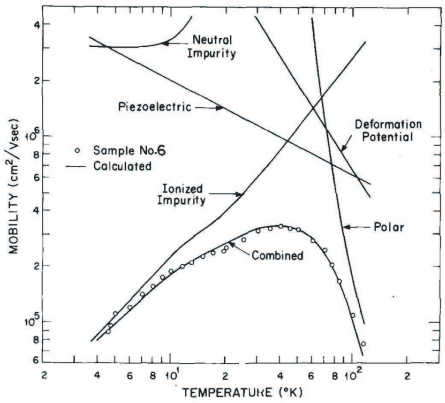

Figure 2.9: Various scattering mechanisms in bulk showing measured (circles) and calculated (curves) mobilities as a function of temperature. The bulk sample had a donor density $n_D = 4.8 \times 10^{19}\,\mathrm{m}^{-3}$ and an acceptor density $n_A = 2.1 \times 10^{10}\,\mathrm{m}^{-3}$ [Stillman 1976].

2.6.2 GaAs 2DEG scattering

Scattering in a 2D electron gas is different from the bulk case because the screening and phase space properties of the electrons are now 2D, while the scattering potentials are still three-dimensional. Decay of the Friedel oscillations in 2D is weaker than in 3D, as mentioned before. Also, new scattering mechanisms arise due to the interface and remote impurities. Relevant mechanisms include:

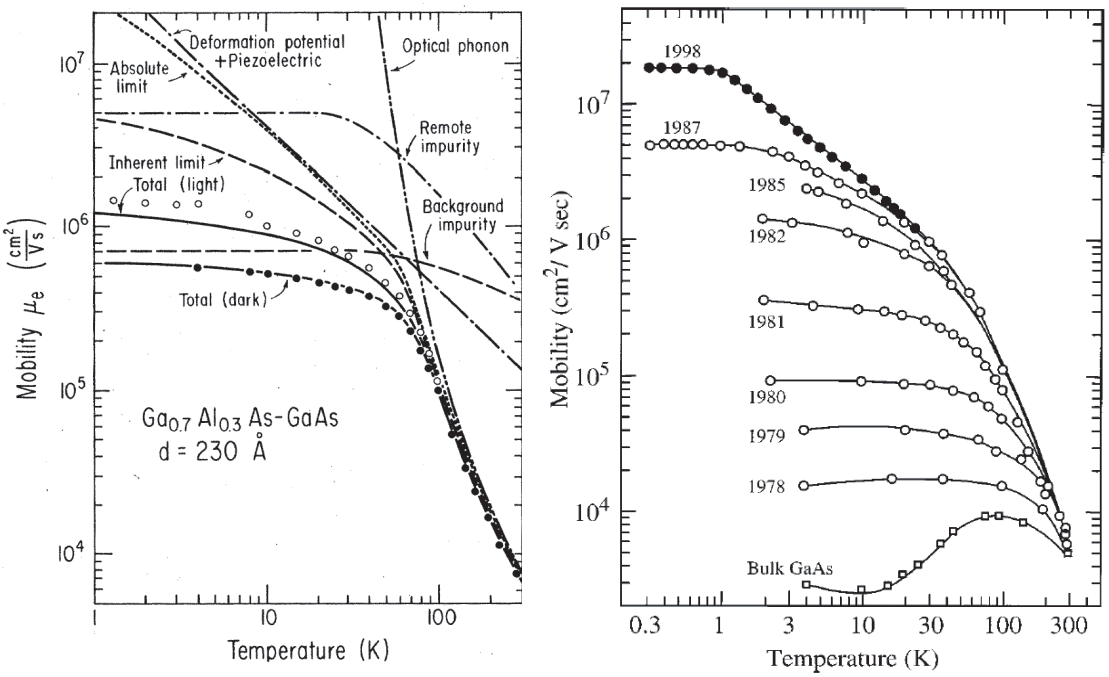

Figure 2.10: Various scattering mechanisms in a *GaAs* 2DEG showing measured (circles) and calculated (curves) mobilities as a function of temperature. The used 2DEG had was measured both in the dark (open circles, $n = 2.2 \times 10^{11}\,\mathrm{cm}^{-2}$) and after illumination (filled circles, $n = 3.8 \times 10^{11}\,\mathrm{cm}^{-2}$), with a spacer thickness $d = 23\,\mathrm{nm}$ and a modulation doping density of $8.6 \times 10^{22}\,\mathrm{m}^{-3}$ distributed evenly within a 20 nm layer between spacer and surface. A homogeneous density of background impurities of $9 \times 10^{19}\,\mathrm{m}^{-3}$ was assumed, a typical number for high quality bulk *GaAs*. [Walukiewicz, 1984]

- *impurities* divided into *remote, ionized donors* that are now spatially separated from the 2DEG by a spacer layer. A small *residual donor density* remains inside the electron gas (and everywhere in the crystal), and can be improved by simply obtaining cleaner materials. Both of these mechanisms can be quite important. Intuitively, one would guess that the farther away the donors are, the lower the scattering they induce is. That is correct, but as the donor layer is further removed from the heteroinferface, the density and thereby mobility in the 2DEG is reduced, unless other parameters are also changed, making further separation of donors from the interface a complicated undertaking.

- *interface roughness* interface imperfections and roughness represents deviation from the perfect crystal and can therefore create scattering. Due to crystal matching, in $GaAs/AlGaAs$ heterostructures this type of scattering is usually very small, unlike the case of the $Si - MOSFET$.

- *alloy scattering* In $Al_xGa_{1-x}As$, 30% of the Ga atoms are replaced by Al, but this occurs in a random, disordered fashion, resulting in a non-periodic potential. For $GaAs$ 2DEG's, the electron wave function almost entirely resides in the crystalline $GaAs$ and only an exponentially small tail protrudes into the $AlGaAs$, making alloy scattering also irrelevant.

- *inherent limit* the mobility that would result in a sample without the background impurities but including the remote donors

2.7 Ohmic Contacts

Despite 40 years of electrical measurements in $GaAs$ and 20 years of 2DEG experiments, making contacts is still not always trivial and the the exact contact mechanism is not completely understood. There are standard recipes that usually work, but depending on the exact structure and application some modifications or fine tuning is often necessary. We define a good ohmic contact to be a source of carriers with a non-zero internal resistance R_c which obeys Ohm's law for all current densities of interest. As discussed previously, a metal on the surface of a $GaAs/AlGaAs$ results normally in a Schottky barrier behaving as a diode, highly non-linear, and certainly not suited as an Ohmic contact. The contact needs to work at the lowest temperatures reached in experiments. In this regime, thermionic currents are negligible, but tunnel currents remain a possibility.

The probability of an electron to tunnel from the semiconductor into the metal depends exponentially on height V_{bi} and width w_d of the barrier and can be estimated in WKB approximation:

$$T(w_d) = \exp\left[-2\int_{w_d}^{0}\left\{\frac{2m^*}{\hbar^2}V(z)\right\}^{1/2}dz\right], \tag{2.7}$$

where $V(z)$ describes the shape of the barrier, with $V(w_d) = 0$. Solving the Poisson equation, we previously found a quadratic dependence on z, see Equation 2.1, which we substitute here into the integral. Further, we determined the width of the barrier, Eq. 2.2. Here we use $\Delta V = e(V - V_{bi})$, with V_{bi} the bias independent barrier height and V an external applied Voltage. The integral is then trivial to compute:

$$T = \exp\frac{e(V - V_{bi})}{\mathcal{E}_0}, \tag{2.8}$$

where we introduced the energy

$$\mathcal{E}_0 = \frac{\hbar}{2}\left(\frac{e^2N}{\epsilon\epsilon_0 m^*}\right)^{1/2} \tag{2.9}$$

characterizing the barrier. $\mathcal{E}_0$ depends on the doping density, and for an achievable doping density $N \sim 10^{25}m^{-3}$ one obtains $\mathcal{E}_0 \sim 60\,\mathrm{meV} \sim 700\,\mathrm{K} \times k$. As before, large doping gives small barrier diameter. The tunneling current density j is then

$$j \propto \left\{1 - \exp\left(\frac{eV}{\mathcal{E}_0}\right)\right\} \approx \frac{eV}{\mathcal{E}_0} + O(V^2) \tag{2.10}$$

where the expansion of the exponent is valid for small Voltages $eV \ll \mathcal{E}_0$. We therefore find ohmic behavior in the small bias range. The factor $\exp(-eV_{bi}/\mathcal{E}_0)$ still multiplies the

entire expression, suppressing the current. Unfortunately, the barrier height cannot be made smaller by a proper choice of metal (surface state density is large). Further, this simple model cannot explain experimentally fabricated ohmic contacts in a satisfactory way.

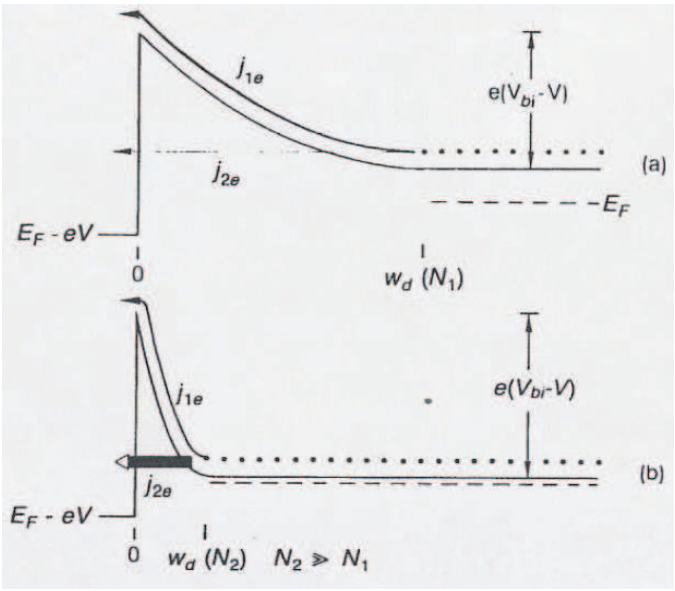

Figure 2.11: upper: doping density N_1, lower: much higher doping $N_2 \gg N_1$. The reduction of the depletion width w_d and consequent increase of the electron tunneling current j_{2e}. [Look 1988]

Many (older) experiments investigating quantum Hall effects have simply used a cleaved square as a sample, without any further processing, and ohmic contacts are made by soldering In onto sample in several places around the perimeter, sometimes followed by a 425 °C anneal, but often without further annealing. Still the most popular metallization for an ohmic contact is composed of Ni, Au and Ge. (Ge is column IV, just below Si). After deposition, the contact is alloyed/thermally annealed by heating up the sample to typically $\sim 400\,°C$ for a few minutes (in order to minimize heating damage, some people use a rapid thermal annealer, where pre-heating and cooling occurs quickly). The metal elements have been seen to mix with the Ga and As in a complicated way, see Figure 2.7 and form new compounds in the process. Sometimes, it appears that spikes of highly doped material are protruding into the $GaAs$, and that the current mainly transfers through these spikes, as illustrated in Figure 2.12. It is thought that the Ni, which wets $GaAs$ very well, acts to prevent "balling up" of the $AuGe$. Variants exist that use nonmagnetic Pt instead of Ni.

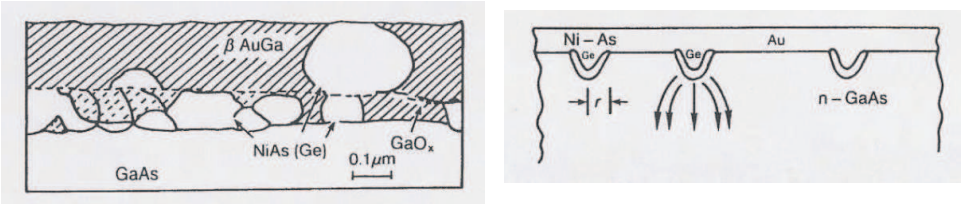

Figure 2.12: left: Various metal phases are present after annealing a $NiAuGe$ contact at 440 °440 for 2 min. right: A model for ohmic contacts in which conduction takes place trough a parallel array of Ge-rich protrusions [Look 1988]

2.8 Schottky gates

When quantum dots and other nanostructures formed in a 2DEG are defined using lateral metal gates (often $TiAu$ or $CrAu$ on the $GaAs$ surface (Ti and Cr act as adhesion layers)), one commonly applies sufficiently negative voltages to deplete electrons underneath gates. Controlling the voltage on the gate controls size of the depletion region and therefore the confinement potential of the device *in situ*. Since this is done in reverse bias of the Schottky diode, the currents flowing through the gates are exceedingly small, which is very important. Appreciable currents flowing from gates (i.e. gate leakage) can completely obliterate the small currents that one would like to measure through the device (in absence of gate leakage), and can also cause heating, decoherence, noise and other undesired effects. This is occasionally an issue due to various problems, but usually, metals make excellent Schottky barriers on the $GaAs$ surfaces or 2DEG materials. $GaAs$ is said to be *gateable*.

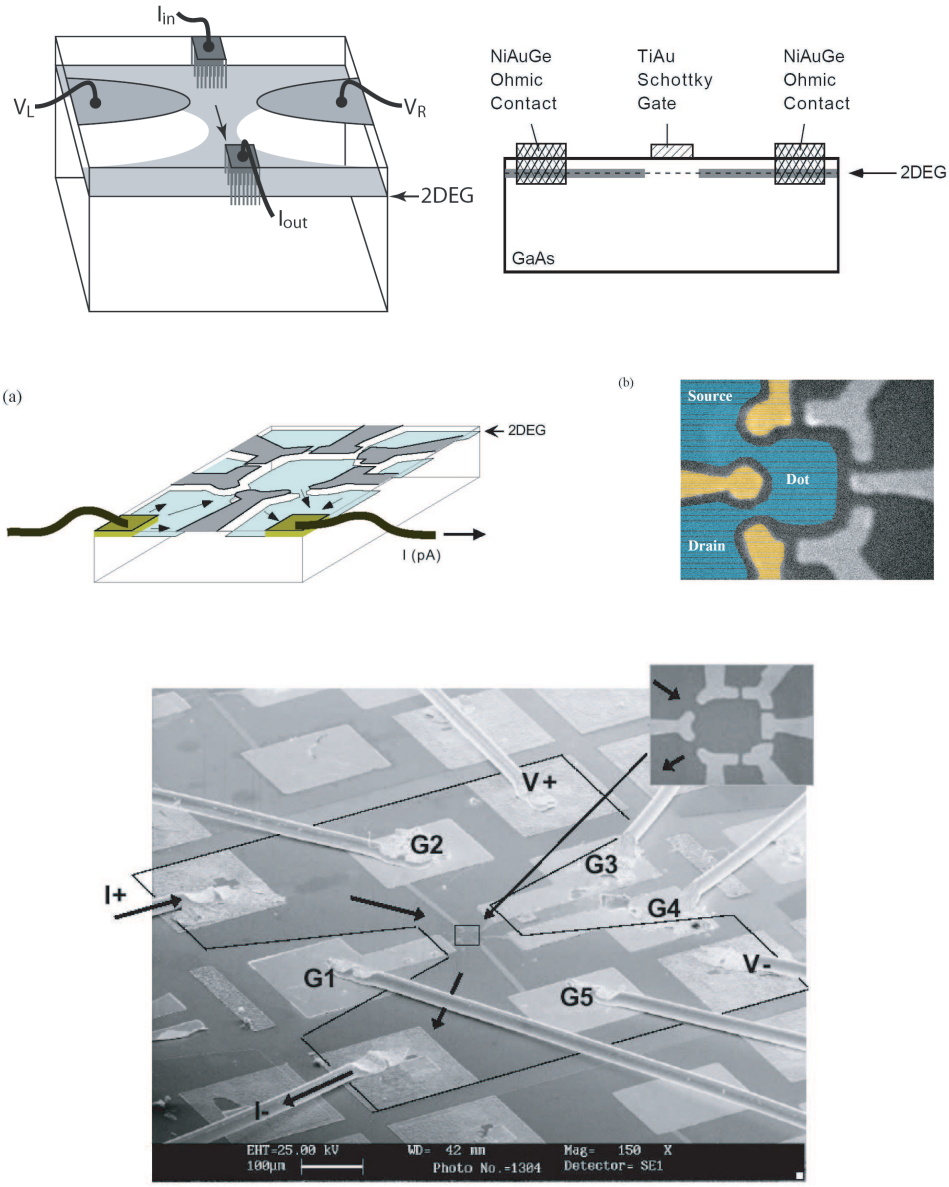

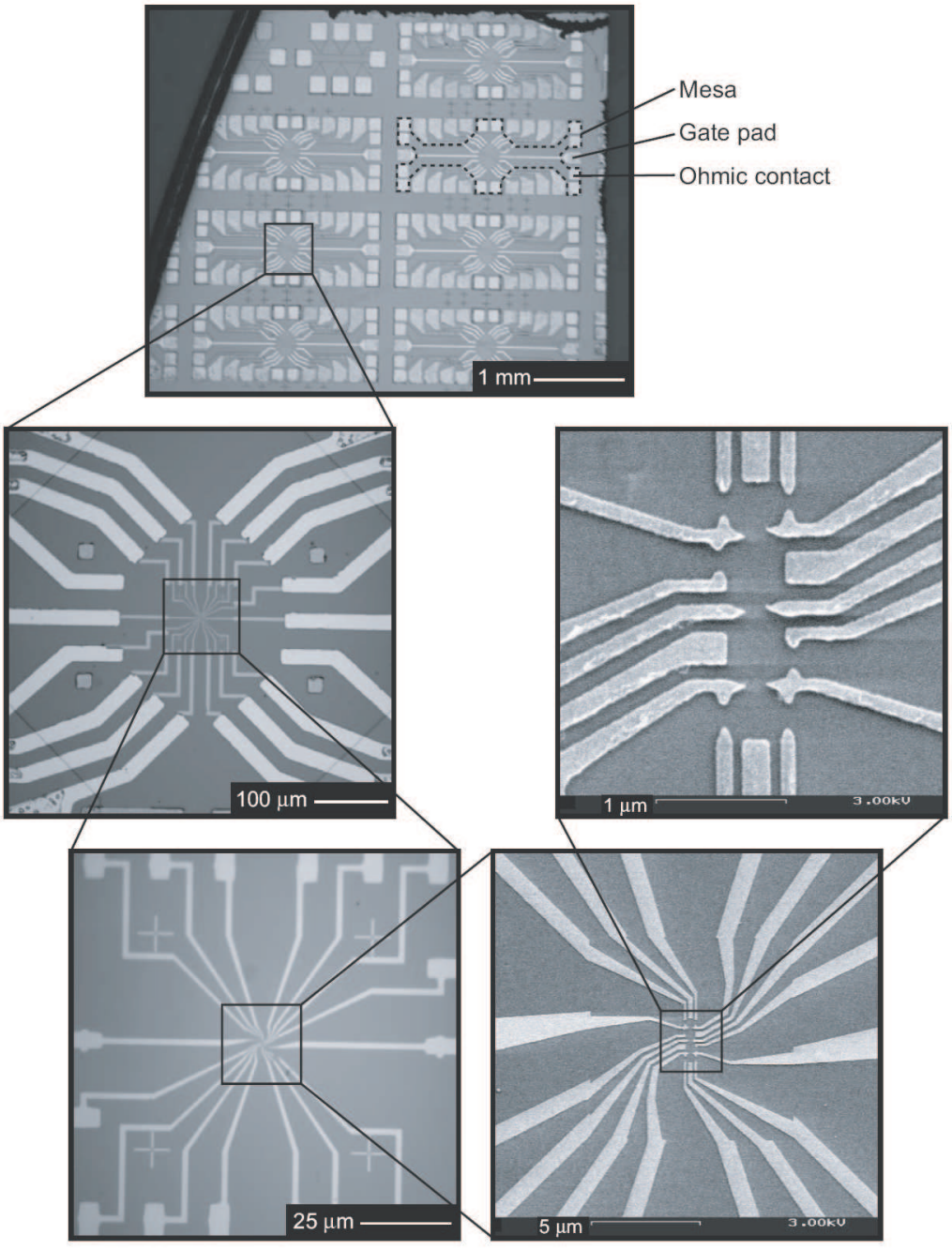
Mesa
Gate pad
Ohmic contact
1 mm
100 µm
1 µm
25 µm
5 µm